Applied Catalysis B: Environmental 111–112 (2012) 246–253

Contents lists available at SciVerse ScienceDirect

Applied Catalysis B: Environmental

journal homepage: www.elsevier.com/locate/apcatb

Simulated solar-light assisted photocatalytic ozonation of metoprolol over titania-coated magnetic activated carbon

Ana Rey[a,*], Diego H. Quiñones[a], Pedro M. Álvarez[a], Fernando J. Beltrán[a], Pawel K. Plucinski[b]

[a] Departamento de Ingeniería Química y Química Física, Universidad de Extremadura, Avenida de Elvas S/N, 06006 Badajoz, Spain
[b] Department of Chemical Engineering, University of Bath, BA2 7AY Bath, United Kingdom

ARTICLE INFO

Article history:
Received 21 July 2011
Received in revised form
26 September 2011
Accepted 4 October 2011
Available online 8 October 2011

Keywords:
Solar photocatalysis
Ozone
Magnetic catalyst
Pharmaceuticals
Water treatment

ABSTRACT

A magnetically separable photocatalyst consisting of magnetic porous activated carbon with attached anatase TiO_2 particles has been prepared and tested for the degradation of metoprolol (MTP) in aqueous solution. The synthesized photocatalyst (TiFeC) was characterized by nitrogen adsorption, XRD, FTIR, SEM, EDX and SQUID magnetometer. The obtained catalyst with a TiO_2 composition of 61 wt.% (mostly anatase) had moderate surface area (BET surface of 331 $m^2\,g^{-1}$) and volume of micropores and exhibited magnetic properties with saturation magnetization of 1.6 emu g^{-1} and neither remanent magnetization nor coercivity. The photocatalytic activity of TiFeC samples was tested by degrading MTP by simulated solar photocatalytic ozonation. The results were compared to those obtained with a commercial titania (Degussa P25) and by photolytic ozonation (i.e., absence of catalyst). Complete MTP removal and more than 60% TOC conversion were achieved after 3 h of photocatalytic ozonation of an aqueous solution containing as much as 50 mg L^{-1} MTP initial concentration. The reusability and stability of the catalyst were tested through a series of five photocatalytic ozonation experiments. Minor amounts of iron and titanium were leached out from the catalyst and the catalytic activity decreased to a very low extent with the reuse of the catalyst.

1. Introduction

Solar photocatalytic detoxification of water and wastewater is an emerging area of research and commercial development as it may be considered as one of the most cost effective treatment technologies in regions of high incoming solar radiation [1,2]. Solar photocatalytic detoxification is a relatively new clean technology to remove toxic and persistent pollutants in water and wastewater by focusing sunlight onto a reactor through which the contaminated water is flowing in the presence of a catalyst. Among candidates for solar photocatalysis, TiO_2 in the form of anatase is the most suitable material for industrial use at present because it is a non-toxic material with high chemical stability, low cost and high oxidation power. It is a semiconductor with a band gap of about 3.2 eV allowing absorption of UV light with wavelengths below 387.5 nm (about 5% of solar spectrum) to generate electron–hole pairs (e^-/h^+) on the catalyst surface. Electron–hole pairs, in turn, trigger a series of reactions generating free-radicals (mainly hydroxyl radicals, $HO^\bullet$), which are very efficient non-selective oxidizers of water pollutants, both chemical compounds and microorganisms (disinfection). Solar TiO_2 photocatalysis is receiving great attention for water and wastewater remediation and it has been extensively investigated for the removal of organic recalcitrant pollutants as for example, pharmaceuticals [3–6], dyes [7] or pesticides [8] as well as to inactivate pathogenic microorganisms such as *Escherichia coli* [9].

Given the concern over the risk posed by the presence of pharmaceutical compounds in water bodies, and hence the possible impacts on public health and aquatic ecosystems a great deal of research is being carried out on technologies for the removal of these compounds [10–12]. In general, pharmaceutical compounds are hardly biodegradable so they are not eliminated by conventional treatment at wastewater treatment plants (WWTPs) and, as a consequence, they are frequently reported to be present in WWTP effluents at ng L^{-1} and even μg L^{-1} concentration levels [13]. Although solar TiO_2 photocatalysis has been found effective for the removal of different pharmaceutical compounds from aqueous solution, to achieve complete mineralization long reaction times are needed because of the formation of a number of intermediates which, frequently, are hard to degrade [2].

In this work, with the aim of enhancing process performance regarding mineralization rate of complex organic molecules such those of pharmaceutical compounds, solar photocatalytic ozonation has been applied. Photocatalytic ozonation, which is the

* Corresponding author. Tel.: +34 924289385; fax: +34 924289385.
E-mail address: anarey@unex.es (A. Rey).

0926-3373/$ – see front matter © 2011 Elsevier B.V. All rights reserved.
doi:10.1016/j.apcatb.2011.10.005

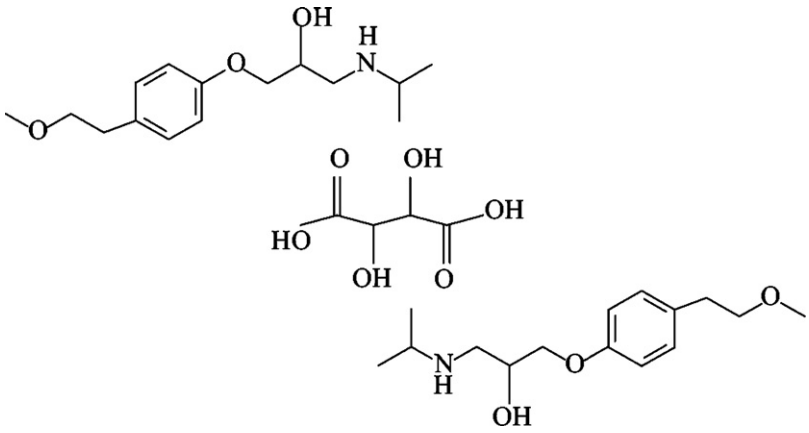

Fig. 1. Molecular structure of metoprolol tartrate.

combination of TiO_2 photocatalysis and ozonation, is a promising advanced oxidation technology capable of producing much larger number of hydroxyl radicals than single ozonation or TiO_2 photocatalysis. In the combined process, the recombination of electron–hole pairs on the TiO_2 surface is reduced with respect to single TiO_2 photocatalysis as electrons are captured by ozone generating a new via of hydroxyl radicals formation and, therefore, increasing the oxidation rate [14,15]. Most of the photocatalytic ozonation studies conducted to date make use of TiO_2 suspensions and UV lamps from low to high pressure [16–18]. In spite of the great degradation rates found for the studied pollutants, two drawbacks of the process can be considered: (1) the use of UV lamps as a source of radiation can make the process expensive for commercial applications; (2) the separation of TiO_2 catalyst in suspension after the reaction is a major obstacle. To overcome these problems, in this work simulated solar radiation has been used as UV light source and a TiO_2 magnetic activated carbon photocatalyst has been synthesized and applied. Literature reports on the preparation of various types of magnetic TiO_2 photocatalysts, which can be easily recovered by the application of an external magnetic field [19–23]. Among them, TiO_2 magnetic activated carbon catalysts have shown a high activity in the photodegradation of phenol and dyes [24,25], but no study has been found on their use in photocatalytic ozonation process.

In this work, we have prepared and characterized a TiO_2 magnetic activated carbon catalyst with enhanced photocatalytic activity to mineralize complex organic pollutants in water such as the pharmaceutical compound metoprolol tartrate (MTP). MTP (see Fig. 1 for structure) is a β-blocker used for several cardiovascular diseases which has been frequently detected in surface waters and effluents from sewage treatment plants [26,27]. The TiO_2 magnetic activated carbon catalyst has been tested in both solar photocatalysis and solar photocatalytic ozonation and compared with the efficiency of commercial TiO_2 powder (Degussa P25), which is a standard material in the field of photocatalytic reactions.

2. Experimental

2.1. Preparation of catalyst

First, a magnetically separable activated carbon (FeC) was prepared following the method reported by Fuertes and Tartaj [28]. In a typical preparation, 10 g of a meso-microporous activated carbon (Darco 12-20, Sigma–Aldrich) were impregnated with 8.7 mL of ferric nitrate (923 g L^{-1}) in ethanol solution to obtain about 12 wt% Fe in the final product. Once the solution was adsorbed onto the activated carbon, the sample was dried at 90 °C for 2 h. After that, it was impregnated with 150 mmol of ethylene glycol. The impregnated activated carbon was then transferred into an oven where it was heated in nitrogen at 350 °C for 2 h. After cooling to room temperature in nitrogen, the magnetic activated carbon sample was milled into powder (d_p < 125 μm).

Titania coated magnetic activated carbon (TiFeC) was prepared by the sol–gel method reported by Ao et al. [24]. First, 25.5 mL of titanium (IV) butoxide (97%, Aldrich) were diluted with 8.2 mL of isopropanol (>99%, Aldrich), and the mixture was added dropwise to 205 mL of distilled water at pH 2 (adjusted with HNO_3 65%, Panreac) under vigorous stirring. The solution was kept under stirring and refluxed at 75 °C for 24 h and, thereafter, transferred to a rotary evaporator where excess alcohol was removed by heating at 80 °C under vacuum, thus obtaining a titania sol. Finally, 3 g of the prepared magnetic activated carbon (FeC) were dispersed in the titania sol and subjected to ultrasonic treatment for 1 h. After evaporation to dryness under vacuum at 80 °C on a rotary evaporator, the residue sample was repeatedly washed with distilled water until no total organic carbon (TOC) was detected in the supernatant and then separated from the liquid fraction by an external magnet to select only the magnetic particles. The TiFeC catalyst thus prepared was dried at 100 °C overnight.

2.2. Catalyst characterization

Surface areas and pore structure of the activated carbon used as support (AC), the magnetic activated carbon (FeC) and the TiFeC catalyst were obtained from nitrogen adsorption–desorption isotherms at −196 °C acquired with a Autosorb 1 apparatus (Quantachrome). Before measurements, the samples were outgassed at 250 °C for 12 h under high vacuum (<10^{-4} Pa). The isotherms were analyzed by BET equation and *t*-plot to obtain BET and external surface areas, respectively. X-ray diffraction (XRD) patterns were collected with a Bruker D8 Advance XRD diffractometer with a CuK_α radiation (λ = 0.1541 nm). The data were collected from $2\theta = 20^\circ$ to 70° at a scan rate of $0.02^\circ\ s^{-1}$ and 1 s per point. FTIR spectra were obtained on a Nicolet iS10 spectrometer using KBr wafers containing about 0.01 g sample. Data were acquired in the wavelength range 400–4000 cm^{-1} using 32 scans with a resolution of 4 cm^{-1}. The morphology of catalyst particles was characterized by scanning electron microscopy (SEM) using a Hitachi S-4800 apparatus working at 20–30 kV accelerating voltage and 500–2000 magnification. In addition, the catalyst was examined by means of energy dispersive X-ray (EDX) analysis to determine the distribution of Ti and Fe in the particles. For that purpose, a SSD detector XFlash 5010 (Bruker), working at 5 kV accelerating voltage and 500–2000 magnification was used. The iron content of the TiFeC catalyst was

Table 1
Properties of the TiFeC catalyst and precursors.

	Fe (wt.%)	TiO_2 (wt.%)	S_{BET} ($m^2\,g^{-1}$)	S_{EXT} ($m^2\,g^{-1}$)	V_{MICRO} ($cm^3\,g^{-1}$)	M_S ($emu\,g^{-1}$)
TiFeC	4.7	61	331	65	0.163	1.56
FeC	12.0	–	552	61	0.253	–
AC	3.7	–	640	51	0.299	–

analyzed by inductively coupled plasma with an ICP-MS NexION 300D (Perkin-Elmer) after acidic microwave digestion of the sample. The amount of TiO_2 on the catalyst was estimated from the mass residue after combustion of the sample in air at 900 °C, taking into account the amount of iron on the sample. Magnetic measurements were performed using a Quantum Design MPMS XL-7 Superconducting Quantum Interference Device (SQUID). The magnetic moment M was measured as function of applied magnetic field H at room temperature.

2.3. Photocatalytic experiments

Photocatalytic experiments were carried out using a commercial solar simulator (Suntest CPS, Atlas) provided with a 1500 W air cooled xenon arc lamp whose emission was restricted to $\lambda > 300$ nm by means of quartz and glass cut-off filters. The irradiation intensity was 550 $W\,m^{-2}$. The chamber of the solar simulator was maintained at about 30 °C throughout the experiments. The experiments were carried out in semi-batch mode using a glass-made agitated tank as reactor provided with gas inlet, gas outlet and liquid sampling ports. Ozone was produced in a laboratory ozone generator (Anseros Ozomat Com AD-02) from pure oxygen and continuously fed to the reactor. In a typical photocatalytic ozonation experiment, the reactor was loaded with 250 mL of an aqueous solution of metoprolol tartrate (>99% Sigma) (MTP) and a given mass of catalyst. The suspension was stirred in the dark for 30 min before switching on the lamp and feeding ozone to the reactor. Ozone (20 $L\,h^{-1}$ gas flow rate and 6 $mg\,L^{-1}$ concentration) was bubbled into the solution through a diffuser placed at the bottom of the reactor. Liquid samples were periodically withdrawn from the reactor and filtered through a 0.2 μm PTFE filter to remove photocatalyst particles prior to analysis. In addition to photocatalytic ozonation experiments using TiFeC, experiments of single adsorption (i.e., absence of radiation and ozone), single ozonation (i.e., absence of radiation and catalyst), catalytic ozonation (i.e., absence of radiation), photolytic ozonation (i.e., absence of catalyst), TiO_2 photocatalysis (i.e., absence of ozone) and photocatalytic ozonation with Degussa P25 (comparative purpose) were carried out. Also photocatalytic experiments varying initial concentration of MTP (10–50 $mg\,L^{-1}$) were completed to examine the effect of contaminant concentration. To test the stability of the TiFeC catalyst, several consecutive experiments were carried out recovering the catalyst particles by using a magnet.

The concentration of MTP was analysed by high-performance liquid chromatography (HP 1100 Series chromatograph) using a Kromasil C-18 column (5 μm, 150 mm long., 4 mm diameter) as stationary phase and 0.65 $mL\,min^{-1}$ of 15:85 acetonitrile:acidic water (0.1% phosphoric acid) as mobile phase. An UV detector set at 225 nm was used for detection. TOC was measured using a Shimadzu TOC-V_{SCH} analyser. Aqueous ozone was measured by following the indigo method [29] using a Helios-α UV/Vis spectrophotometer set at 600 nm. Ozone in the gas phase was continuously monitored by means of an Anseros Ozomat GM-6000Pro analyser. Iron and titanium in solution were analysed by means of inductively coupled plasma using a Perkin Elmer NexION 300D ICP-MS apparatus.

3. Results and discussion

3.1. Characterization of TiO_2 magnetic activated carbon

Table 1 summarizes composition, some textural parameters (BET and external surface areas) and saturation magnetization of the prepared TiFeC catalyst, the impregnated activated carbon (FeC) and the activated carbon used as support itself. It can be seen that the TiO_2 mass composition of the TiFeC catalyst is somewhat lower than expected (i.e., 66 wt.%) likely due to the loss of some TiO_2 during the washing steps of the synthesis procedure. The amount of iron in the TiFeC catalyst, about 5 wt.%, is in good agreement with the Fe mass composition of the activated carbon used as support and the amount of iron added during the preparation of the magnetically separable activated carbon (FeC).

Fig. 2 shows the nitrogen adsorption–desorption isotherms of the activated carbon support and the FeC and TiFeC samples. All the three samples show a typical type I isotherm characteristic of microporous materials with high uptake at very low relative pressures [30]. However, a drastic decrease in the volume adsorbed at low relative pressures was produced after impregnation (FeC sample) and TiFeC catalyst preparation. As a result, noticeable decreases in BET surface area and micropore volume were computed (see Table 1). Such a loss of internal surface was most likely due to the blockage of some microporous as a consequence of iron species and TiO_2 deposition [24]. The activated carbon used as support had a significant external surface area which was even increased upon TiFeC preparation likely due to the formation of new large pores (meso or macropores) by the aggregation of titania particles on the support.

Fig. 3 shows the XRD patterns of the activated carbon support and the TiFeC catalyst. In the diffractogram of the activated carbon (AC) two broad peaks at $2\theta = 26°$ and 43° can be distinguished corresponding to characteristic graphite diffraction peaks. The peaks width, which is characteristic of amorphous carbon

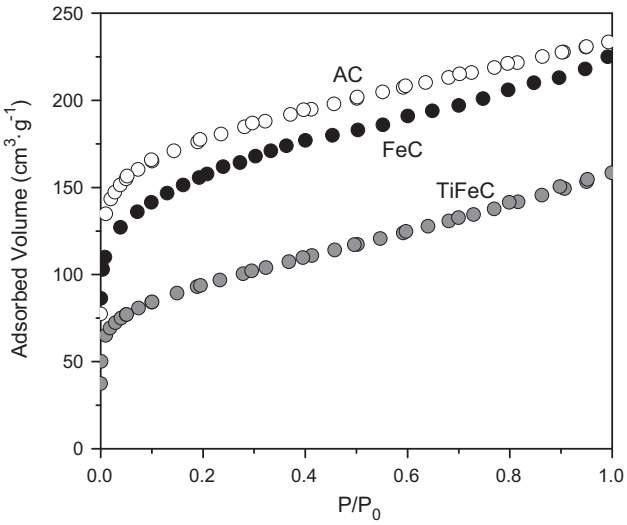

Fig. 2. N_2 adsorption–desorption isotherms of AC support, FeC and TiFeC catalysts.

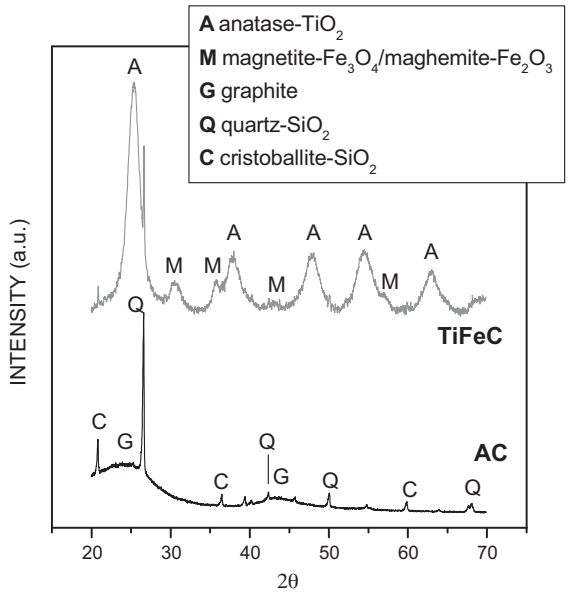

Fig. 3. XRD patterns of the AC support and TiFeC catalyst.

materials, together with the absence of other (*h k l*) peaks suggests low dimensions of the graphitic domains. It can also be noticed the presence of a sharp diffraction peak at 26.6° corresponding to SiO_2-quartz reflection, and others at 21.9°, 36.0° and 62.0° which are likely due to SiO_2–cristoballite structures. XRD pattern of the TiFeC sample shows the characteristic peaks of anatase at 25.4°, 38.0°, 48.0°, 54.7° and 63.0°. From the (1 0 1) peak the anatase crystallite size was calculated to be 4.7 nm after application of the Scherrer equation. Regarding the structure of iron species present in the catalyst, very small and wide characteristic diffraction peaks (30.4°, 35.7°, 43.4° and 57.4°) of magnetite or maghemite can be observed. In fact, both iron species have very similar XRD patterns so the XRD results do not allow one to distinguish one species from another. Finally, some SiO_2 peaks can also be observed in the diffractogram of TiFeC.

Fig. 4 shows the FTIR spectra recorded for activated carbon and TiFeC samples. In the spectrum of activated carbon (AC), the broad band in the 3200–3600 cm^{-1} region can be assigned to the

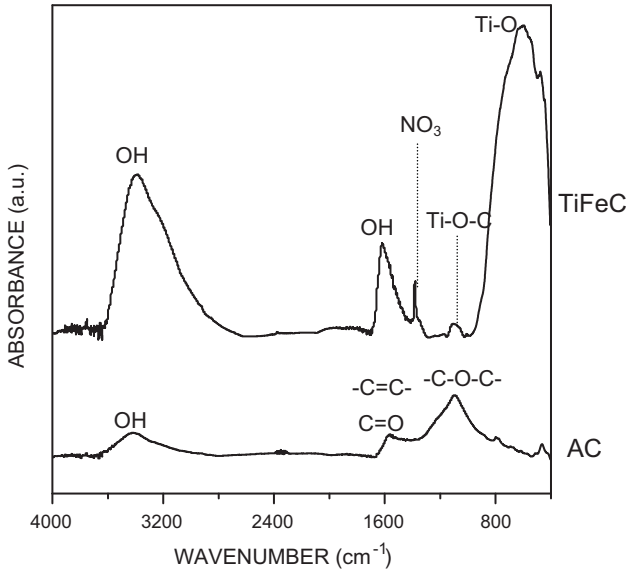

Fig. 4. FTIR spectra of the AC support and TiFeC catalyst.

stretching vibration of –OH groups present as phenolic surface groups [31]. In the TiFeC sample this band is also attributable to TiO_2–OH bonds [32,33]. The AC sample exhibits overlapped bands in the region 1700–1550 cm^{-1} which are generally accepted to be due to absorption of quinone and other carbonyl groups (–C=O structures) and stretching vibration of aromatic structures [31]. The broad band centred at about 1100 cm^{-1} in the spectrum of the activated carbon can be assigned primarily to ether structures (–C–O–C–) [31,34]. In the TiFeC spectrum, the broad band observed at 600 cm^{-1} can be due to Ti–O stretching vibration and the peak at 1620 cm^{-1} may correspond to bending vibration of OH groups of adsorbed water [35]. The sharp peak that can be seen at 1385 cm^{-1} it is ascribable to the presence of nitrates ($-NO_3^-$) on the catalyst surface [36], which would had been incorporated from the iron precursor during the synthesis of FeC. Finally, the peak located at 1085 cm^{-1} could be assigned to Ti–O–C structures, suggesting a conjugation effect between bulk activated carbon and Ti–O bonds [37].

The morphology of the catalyst particles has been investigated by SEM. Fig. 5 (left) shows the SEM images at two different magnifications. It can be observed the non-uniform size of the catalyst particles, which were in any case lower than 125 μm. The distribution of the Fe and Ti species was analysed by means of energy dispersive X-ray (EDX) analysis by scanning the same area as shown in SEM images. Mapping results are shown in Fig. 5 (right) where yellow and red areas correspond to Ti and Fe species, respectively. From these figures it is apparent a uniform distribution of iron on the catalyst particles, whereas titanium was present in most of the particles with a less uniform concentration.

Fig. 6 illustrates the magnetization curve of the TiFeC catalyst. From it the value of saturation magnetization (M_S) was calculated to be 1.56 emu g^{-1}. This value is similar to that reported by Ao et al. [24]. However the saturation magnetization expected if all the iron was as magnetite was 5.97 emu g^{-1} taking into account the catalyst composition (Fe 4.7 wt.%) and the saturation magnetization of bulk magnetite (92 emu g^{-1}). This fact suggests that a large amount of the iron incorporated to the catalyst is in a form other than magnetite. Nevertheless the catalyst could be easily separated from the solution with an external magnet as it has been illustrated in Fig. 6 (right). The sample showed almost zero coercivity and zero remanent magnetization, which indicates superparamagnetic behaviour of the catalyst particles. Accordingly, the particles did not aggregate being separated by a magnet and could be easily re-dispersed in solution for reusing.

3.2. Photocatalytic activity

3.2.1. Photodegradation of MTP

Fig. 7A shows the evolution of MTP dimensionless concentration with time during the course of selected experiments. Two regions can be seen in the figure. First, a 30 min stage designated as dark stage (absence of radiation) where only adsorption onto the catalyst took place, followed by a second stage where adsorption and/or oxidation reactions developed. From the adsorption curve it can be observed that about 25–30% of the MTP initially present in the aqueous solution was adsorbed onto the TiFeC catalyst at adsorption equilibrium. Also it can be seen that at the end of the dark stage, the concentration of MTP was close to the adsorption equilibrium value. Photocatalytic oxidation (TiFeC in the absence of ozone but radiation and oxygen) led to about 46% MTP removal after 2 h of irradiation while complete MTP removal was observed after 40 min reaction time in all the experiments when using ozone since this reacts relatively fast with MTP ($k_{O_3} = 1.4 \times 10^3$ M^{-1} s^{-1} at pH 7 [38]). Moreover, MTP concentration profiles were quite similar for single ozonation, catalytic ozonation and photocatalytic ozonation,

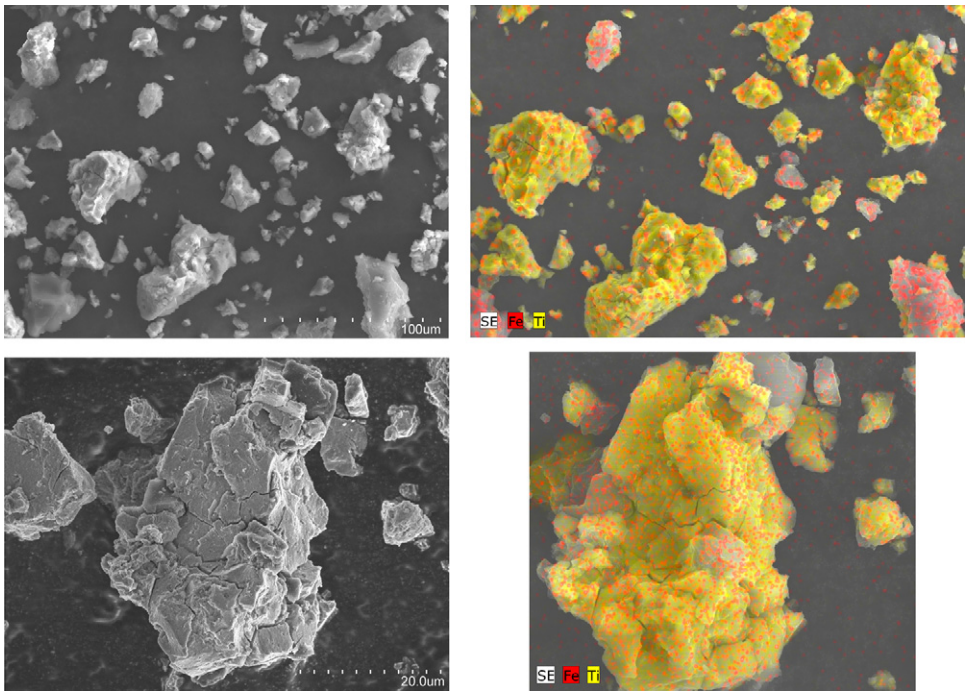

Fig. 5. SEM images (left) and EDX mapping (right) for the TiFeC catalyst.

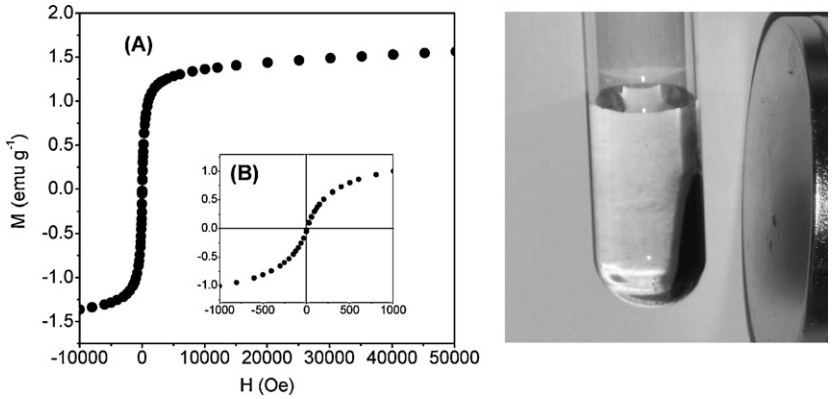

Fig. 6. Magnetization vs. applied magnetic field at 25 °C of TiFeC catalyst (left A) and (B) zoom of the −1000 to 1000 range. Illustration of the catalyst separation with a magnet (right).

suggesting that in these experiments MTP was mainly removed through direct ozonation reactions with little catalytic effect.

Table 2 shows the pseudo-first order apparent rate constant derived from Fig. 7A. In agreement with the discussion above, it can be seen that k_{app} for the photocatalytic process (absence of ozone) was much lower than those for the ozone-based processes.

In Fig. 7A the results of MTP degradation from a photocatalytic ozonation experiment with Degussa P25 are also shown. It is apparent that the catalytic activity of Degussa P25 was somewhat higher than that of the synthesized TiFeC catalyst. Thus, the computed k_{app} was 1.5 times higher for the P25 catalyzed process. Surprisingly, MTP removal by photolytic ozonation was faster than those achieved by any of the photo-catalyzed systems. This fact can be explained by partial decomposition of ozone into hydroxyl radicals by photolysis at wavelengths near 300 nm [39].

Ozone consumptions within the processes are reported in Table 3. The presented data are the amounts of ozone consumed per mole of MTP degraded at 50% MTP removal, 98% MTP removal,

Table 2
Experimental pseudo-first order apparent rate constants for MTP depletion.

Process	k_{app} (min^{-1})	R^2
Photocatalysis	0.005	0.97
Ozonation	0.121	0.98
Catalytic ozonation	0.110	0.98
Photolytic ozonation	0.319	0.99
Photocatalytic ozonation (TiFeC)	0.137	0.97
Photocatalytic ozonation (P25)	0.201	0.99

Table 3
Ozone consumption during all the O_3-treatments with 10 mg L^{-1} MTP initial concentration.

Process	O_3 consumed/MTP degraded (mol/mol)		
	MTP 50%	MTP 98%	TOC 50%
Ozonation	2.26	6.29	–
Catalytic ozonation	3.70	8.74	1.68
Photolytic ozonation	3.42	5.24	1.43
Photocatalytic ozonation (TiFeC)	4.11	7.69	1.14
Photocatalytic ozonation (P25)	1.23	3.32	0.67

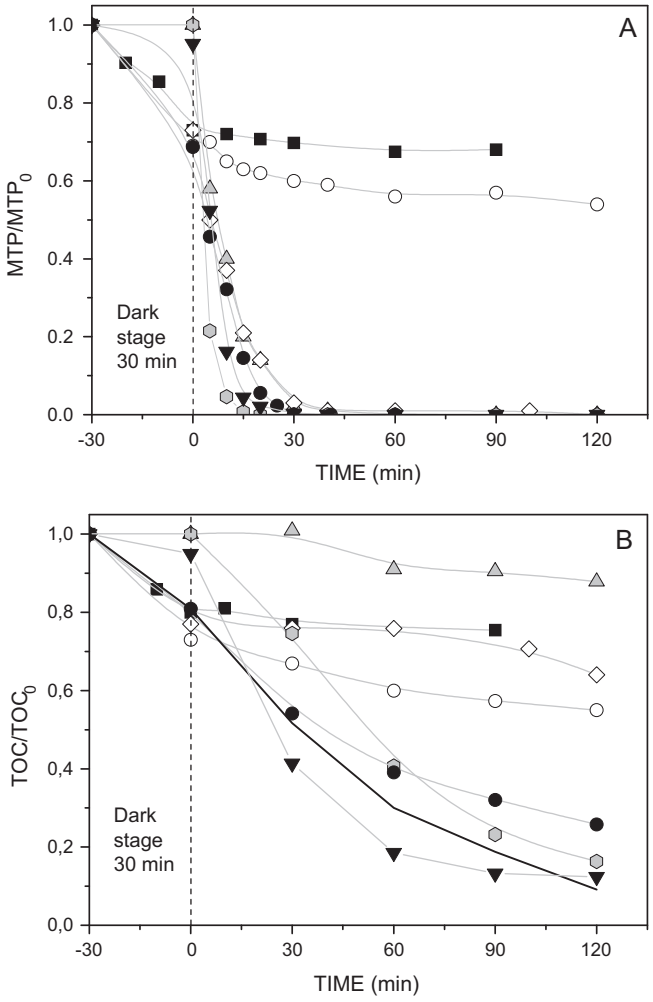

Fig. 7. Variation of MTP (A) and TOC (B) dimensionless concentration with time. Conditions: $C_{MTP0} = 10\,mg\,L^{-1}$, $^*C_{TiO_2} = 0.25\,g\,L^{-1}$ ($C_{CAT} = 0.375\,g\,L^{-1}$), gas flow rate: $20\,L\,h^{-1}$, $pH_0 = 6.5$, $T = 30^\circ C$, $^*C_{O_3g} = 6\,mg\,L^{-1}$ (*in the corresponding experiments). Symbols: (■) adsorption, (○) photocatalysis, (△) ozonation, (◊) catalytic ozonation, (⬡) photolytic ozonation, (●) photocatalytic ozonation, (▼) P25-photocatalytic ozonation, (–) photocatalytic ozonation corrected.

and per mole of carbon at 50% TOC removal. From this table it is apparent that the least ozone-consuming process was the photocatalytic ozonation with Degussa P25. In fact, the amount of ozone used was about three times higher for the photocatalytic ozonation with TiFeC than with Degussa P25. This result suggests that in the presence of TiFeC much ozone is consumed through parallel reactions (i.e., ozonation of MTP by-products and catalyst surface oxidation) while Degussa P25 was a more efficient photocatalyst for degrading MTP by ozonation.

Regarding mineralization, Fig. 7B shows the time evolution of dimensionless TOC during the course of experiments. While single ozonation, single adsorption, catalytic ozonation and photocatalytic oxidation (without ozone) led to less than 50% TOC removal after 2 h of experiment, greater mineralization levels were achieved by photocatalytic ozonation both with TiFeC or Degussa P25 and photolytic ozonation. It can be hypothesized that under the conditions studied, during photocatalytic ozonation hydroxyl radicals are formed on the photocatalyst surface [16]. Thus, intermediates from MTP ozonation could, in turn, be most efficiently oxidized by hydroxyl radicals resulting in an enhanced mineralization [40].

It is important to recall here that a powdered carbon material subjected to ozonation in water may release organic carbon to water because of the reaction between ozone and surface groups of the activated carbon [41]. To assess whether or not TOC release was produced in our photocatalytic ozonation experiments with TiFeC, some experiments were carried out in ultrapure water (without MTP). TOC concentrations up to $1.5\,mg\,L^{-1}$ were detected but this organic carbon is expected not to be an environmental problem because of its non-toxic nature and the fact that it can be removed by further ozonation [41]. In Fig. 7B the TOC profile for the TiFeC photocatalytic ozonation process has been re-plotted (solid line) by subtracting the TOC released from the actual TOC profile so that only the effect on MTP mineralization is shown. It can be seen now, that the photocatalytic effect of TiFeC on MTP mineralization was only slightly lower than that of Degussa P25.

From Fig. 7B it is also observed that great MTP mineralization was also achieved by photolytic ozonation (absence of catalyst). In a previous work, using a high-pressure mercury lamp with effective irradiation at 313 nm, high mineralization of the antibiotic sulfamethoxazole was also achieved by photolytic ozonation [42]. Up to the best of our knowledge the degradation of water pollutants by solar photolytic ozonation has not been yet studied. Given the promising results obtained in this work it will be a subject of further work.

3.2.2. *Influence of initial MTP concentration*

In order to study the effect of MTP initial concentration, some experiments (photocatalytic ozonation and photolytic ozonation) were carried out with 10 and $50\,mg\,L^{-1}$ initial concentration of MTP. The time profiles of these experiments are depicted in Fig. 8A for MTP and Fig. 8B for TOC. As expected, higher reaction times were needed to reach complete MTP removal when using $50\,mg\,L^{-1}$ MTP initial concentration. Regardless of the initial concentration used, MTP removal rates achieved by photocatalytic ozonation and photolytic ozonation were close to each other. However, regarding TOC degradation, while no great differences were observed at $10\,mg\,L^{-1}$ initial concentration, at $50\,mg\,L^{-1}$ initial concentration TOC degradation was faster by photocatalytic ozonation. Thus, for example TOC conversions after 3 h were 34% and 64% for photolytic ozonation and photocatalytic ozonation, respectively. Therefore, it can be concluded that the TiFeC catalyst enhanced the mineralization rate of MTP during photocatalytic ozonation in comparison to the photolytic ozonation.

3.2.3. *Catalyst stability and reusability*

One of the key factors for the practical application of heterogeneous photocatalytic processes in water treatment is the recovery and reusability of the catalyst after the treatment. In this line, five consecutive runs were carried out with the TiFeC catalyst. In these experiments, $50\,mg\,L^{-1}$ MTP initial concentration was used. After each 2-h run, the catalyst was separated with a magnet and the aqueous solution was removed from the reactor and replaced by a fresh MTP aqueous solution. Fig. 9 shows some of the results obtained in terms of MTP and TOC conversions. First, it is seen that the adsorption capacity of the catalyst was barely affected throughout the series of experiments. Thus, MTP removed by adsorption during the initial dark stage was around 25% though slightly lower for the 4th and 5th run. This suggests that after each run the catalyst is free of adsorbed MTP which has been degraded by surface oxidation reactions. However, after a number of cycles some reaction by-products could remain on the catalyst surface, thus preventing MTP adsorption to some extent. Also, MTP conversion after 2 h, was kept practically constant around 95–98% for the whole series of experiments. However, TOC conversion decreased from 43% reached in the first run to 30–35% in the subsequent experiments, being always higher than the TOC conversion reached in a photolytic ozonation experiment (about 20%). Also, the amounts of Fe and Ti leached out from the catalyst were measured. Table 4

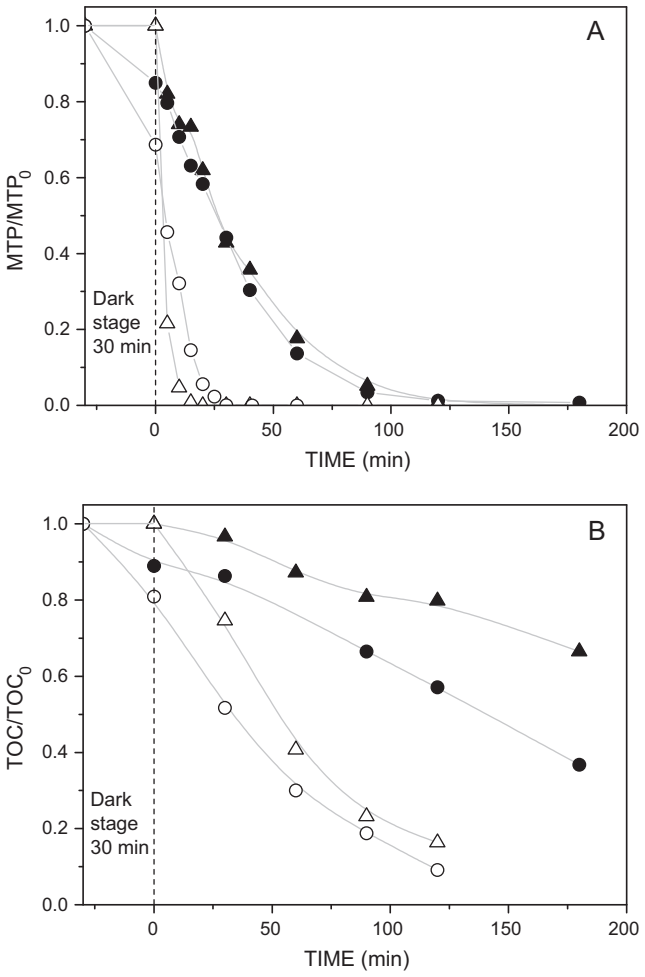

Fig. 8. Variation of MTP (A) and TOC (B) dimensionless concentration with time. Conditions: C_{MTP0} = 50 mcg L^{-1} (▲ photolytic ozonation, ● photocatalytic ozonation) and 10 mg L^{-1} (△ photolytic ozonation, ○ photocatalytic ozonation), $^{*}C_{TiO_2}$ = 0.25 g L^{-1} (C_{CAT} = 0.375 g L^{-1}), gas flow rate: 20 L h^{-1}, pH_0 = 6.5, T = 30 °C, C_{O_3g} = 6 mg L^{-1} (*in the corresponding experiments).

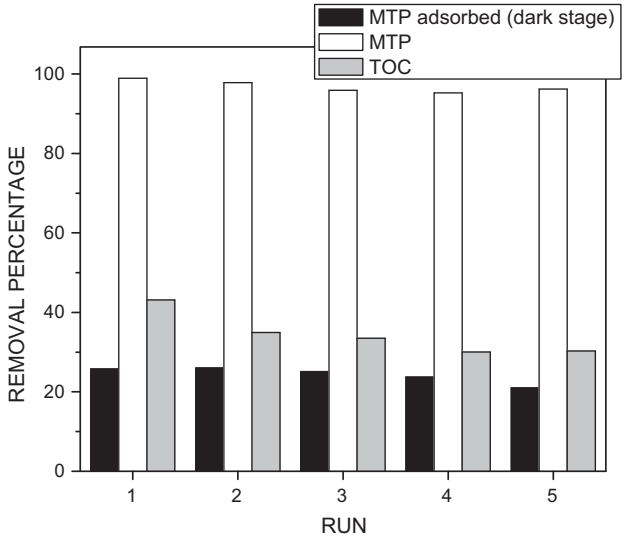

Fig. 9. Initial adsorption, MTP and TOC conversion for consecutive photocatalytic ozonation runs with TiFeC catalyst. Conditions: C_{MTP0} = 50 mg L^{-1}, C_{TiO_2} = 0.25 g L^{-1} (C_{CAT} = 0.375 g L^{-1}), gas flow rate: 20 L h^{-1}, pH_0 = 6.5, T = 30° C, C_{O_3g} = 6 mg L^{-1}.

Table 4
Ti and Fe lixiviation during photocatalytic ozonation runs with TiFeC catalyst.

Run	1	2	3	4	5
Ti (μg L^{-1})	<15	<10	<10	<10	<15
Fe (μg L^{-1})	<25	<20	<20	<20	<20

shows the element concentrations found in solution after each run. It can be seen that both Fe and Ti concentrations were low. Thus, from mass balances it was calculated that the percentages of titanium and iron leached out from the catalyst after the whole series of consecutive experiments were lower than 0.04% and 0.60%, respectively.

4. Conclusions

This study focuses on the preparation of a titania-coated magnetic activated carbon (TiFeC) to be used in the removal of emerging contaminants from water by solar photocatalytic methods. The synthesized catalyst showed moderate surface areas and pore volume which allow adsorption of organic compounds to some extent. TiO_2 crystallites attached to the activated carbon were in the form of anatase, thus showing high photocatalytic activity. Given its magnetic properties, catalyst particles were demonstrated to be easily separable by a magnet. Metoprolol (MTP) was chosen as model pollutant to test the photocatalytic activity of the synthesized catalyst. Solar photocatalytic ozonation resulted in higher MTP removal rate and TOC degradation than single adsorption, single ozonation and solar photocatalysis without ozone. However, solar photolytic ozonation (without catalyst) effectiveness was comparable to that of solar photocatalytic ozonation when using a MTP initial concentration of 10 mg L^{-1}. Given this promising result, new research is being carried out in the application of solar photolytic ozonation for the degradation of other emerging contaminants and elucidation of reaction mechanisms. The TiFeC catalyst showed good stability (low Fe and Ti losses) and reusability. Although the TiFeC catalyst was not as effective as Degussa 25 TiO_2, its easy separation by an external magnetic field makes it an interesting alternative material for solar photocatalytic processes.

Acknowledgements

This work has been financed by the Spanish Ministerio de Ciencia e Innovación (MICINN) and European Feder Funds through the project CTQ2009-13459-C05-05/PPQ. Authors acknowledge the SAIUEX service of the University of Extremadura for the characterization analyses. A. Rey thanks the University of Extremadura for a post-doctoral research grant. D.H. Quiñones thanks the MICINN for a FPI grant.

References

[1] J. Blanco-Gálvez, P. Fernández-Ibañez, S. Malato-Rodríguez, J. Sol. Energy Eng. 129 (2007) 4–15.
[2] S. Malato, P. Fernández-Ibañez, M.I. Maldonado, J. Blanco, W. Gernjak, Catal. Today 141 (2009) 1–59.
[3] S. Malato, J. Cáceres, A. Agüera, M. Mezcua, D. Hernando, J. Vial, A.R. Fernández-Alba, Environ. Sci. Technol. 35 (2001) 4359–4366.
[4] F. Méndez-Arriaga, S. Esplugas, J. Giménez, Water Res. 42 (2008) 585–594.
[5] T.E. Doll, F.H. Frimmel, Water Res. 39 (2005) 403–411.
[6] N. Miranda-García, S. Suárez, B. Sánchez, J.M. Coronado, S. Malato, M.I. Maldonado, Appl. Catal. B: Environ. 103 (2011) 294–301.
[7] B. Neppolian, H.C. Choi, S. Sakthivel, B. Arabindoo, V. Murugesan, Chemosphere 46 (2002) 1173–1181.
[8] A. Arques, A.M. Amat, A. García-Ripoll, R. Vicente, J. Hazard. Mater. 146 (2007) 447–452.
[9] F.M. Salih, J. Appl. Microbiol. 92 (2002) 920–926.
[10] S. Baumgarten, H.F. Schroder, C. Charwath, M. Lange, S. Beier, J. Pinnekamp, Water Sci. Technol. 56 (2007) 1–8.

[11] O.K. Dalrymple, D.H. Yeh, M.A. Trotz, J. Chem. Technol. Biotechnol. 82 (2007) 121–134.
[12] K. Ikehata, N.J. Naghashkar, M.G. El-Din, Ozone Sci. Eng. 28 (2006) 353–414.
[13] R. Rosal, A. Rodriguez, J.A. Perdigon-Melon, A. Petre, E. Garcia-Calvo, M.J. Gomez, A. Aguera, A.R. Fernandez-Alba, Water Res. 44 (2010) 578–588.
[14] T.E. Agustina, H.M. Ang, V.K. Vareek, J. Photochem. Photobiol. C: Photochem. Rev. 6 (2005) 264–273.
[15] V. Augugliaro, M. Litter, L. Palmisano, J. Soria, J. Photochem. Photobiol. C: Photochem. Rev. 7 (2006) 127–144.
[16] F.J. Beltrán, A. Aguinaco, J.F. García-Araya, Water Res. 43 (2009) 1359–1369.
[17] O. Gimeno, F.J. Rivas, F.J. Beltrán, M. Carbajo, J. Agric. Food Chem. 55 (2007) 9944–9950.
[18] R. Rajeswari, S. Kanmani, J. Adv. Oxid. Technol. 12 (2009) 208–214.
[19] D. Beydoun, R. Amal, G.K.C. Low, S. McEvoy, J. Phys. Chem. B 104 (2000) 4387–4396.
[20] D. Beydoun, R. Amal, Mater. Sci. Eng. 94 (2002) 71–81.
[21] S. Watson, J. Scott, D. Beydoun, R. Amal, J. Nanopart. 7 (2005) 691–705.
[22] S. Xu, W. Shangguan, J. Yuan, M. Chen, J. Shi. Appl. Catal. B: Environ. 71 (2007) 177–184.
[23] P.M. Álvarez, J. Jaramillo, F. López-Piñero, P.K. Plucinski, Appl. Catal. B: Environ. 100 (2010) 338–345.
[24] Y. Ao, J. Xu, D. Fu, C. Yuan, Carbon 46 (2008) 596–603.
[25] S. Wang, S. Zhou, Appl. Surf. Sci. 256 (2010) 6191–6198.
[26] V. Romero, N. de la Cruz, R.F. Dantas, P. Marco, J. Giménez, S. Esplugas, Catal. Today 161 (2011) 115–120.
[27] V. Contardo-Jara, S. Pflugmacher, G. Nützmann, W. Kloas, C. Wiegand, Environ. Pollut. 158 (2010) 2059–2066.
[28] A.B. Fuertes, P. Tartaj, Chem. Mater. 18 (2006) 1675–1679.
[29] H. Bader, J. Hoigné, Water Res. 15 (1981) 449–456.
[30] S. Brunauer, L.S. Deming, W.S. Deming, E. Teller, J. Am. Chem. Soc. 62 (1940) 1723.
[31] P. Serp, J.L. Figueiredo, Carbon Materials for Catalysis, John Wiley and Sons, INC, 2009, pp. 63–66.
[32] T. López, J.A. Moreno, R. Gómez, X. Bokhimi, J.A. Wang, H. Yee-Madeira, G. Pecci, P. Reyes, J. Mater. Chem. 12 (2002) 714–718.
[33] H. Jensen, A. Soloviev, Z. Li, E.G. Sogaard, Appl. Surf. Sci. 246 (2005) 239–249.
[34] L.R. Radovic (Ed.), Chemistry and Physics of Carbon, A Series of Advances, vol. 27, Marcel Dekker Inc., New York, 2001, pp. 131–137.
[35] Y. Suda, T. Morimoto, Langmuir 3 (1987) 786–788.
[36] M. Pakula, A. Swiatkowski, M. Walczyk, S. Biniak, Colloids Surf. A: Physicochem. Eng. Aspects 260 (2005) 145–155.
[37] S.X. Liu, X.Y. Chen, X. Chen, J. Hazard. Mater. 143 (2007) 257–263.
[38] F.J. Benitez, J.L. Acero, F.J. Real, G. Roldán, Chemosphere 77 (2009) 53–59.
[39] H. Taube, Trans. Faraday Soc. 53 (1957) 656–665.
[40] J. Benner, T.A. Ternes, Environ. Sci. Technol. 43 (2009) 5472–5480.
[41] J.P. Pocostales, P.M. Álvarez, F.J. Beltrán, Chem. Eng. J. 164 (2010) 70–76.
[42] F.J. Beltrán, A. Aguinaco, J.F. García-Araya, A. Oropesa, Water Res. 42 (2008) 3799–3808.